

1 **Developmental Circadian Disruption Alters Placental Signaling in Mice**

2

3 Danielle A. Clarkson-Townsend^{1,2}, Katie L. Bales^{2,3}, Karen E. Hermetz¹, Amber A. Burt¹,
4 Mabelle T. Pardue^{2,4}, Carmen J. Marsit^{1*}

5

6 ¹*Gangarosa Department of Environmental Health, Rollins School of Public Health, Emory*
7 *University, Atlanta, GA, USA*

8

9 ²*Center for Visual and Neurocognitive Rehabilitation, Atlanta VA Healthcare System, Decatur,*
10 *GA, USA*

11

12 ³*Department of Ophthalmology, Emory University, Atlanta, GA, USA*

13

14 ⁴*Department of Biomedical Engineering, Georgia Institute of Technology and Emory University,*
15 *Atlanta, GA, USA*

16

17 *Correspondence: Carmen Marsit, Department of Environmental Health, Emory University

18 **Email:** carmen.j.marsit@emory.edu

19 **Mailing address:** 8009 Claudia Nance Rollins Building, Emory University Rollins School of
20 Public Health, 1518 Clifton Road, Atlanta, GA 30322

21 **Phone:** (404) 727-8744

22 **Abstract**

23 Circadian disruption has been largely overlooked as a developmental exposure. The placenta, a
24 conduit between the maternal and fetal environments, may relay circadian cues to the fetus. We
25 have previously shown that developmental chronodisruption causes visual impairment and
26 increased retinal microglial and macrophage marker expression. Here, we investigated the
27 impacts of environmental circadian disruption on fetal and placental outcomes in a C57BL/6J
28 mouse (*Mus musculus*) model. Developmental chronodisruption had no effect on embryo count,
29 placental weight, or fetal sex ratio. When measured with RNAseq, mice exposed to
30 developmental circadian disruption (CD) had differential placental expression of several
31 transcripts including *Serpinfl*, which encodes pigment-epithelium derived factor (PEDF).
32 Immunofluorescence of microglia/macrophage markers, Iba1 and CD11b, also revealed
33 significant upregulation of immune cell markers in CD-exposed placenta. Our results suggest
34 that *in utero* circadian disruption enhances placental immune cell expression, potentially
35 programming a pro-inflammatory tissue environment that increases the risk of chronic disease in
36 adulthood.

37

38 *Keywords:* placenta, developmental chronodisruption, circadian disruption, developmental
39 programming, DOHaD

40

41 **Abbreviations:**

42 BH, Benjamini and Hochberg

43 CL, control light

44 CD, circadian disruption

45 DOHaD, Developmental Origins of Health and Disease

46 INTRODUCTION

47 Environmental light exposure has changed rapidly over the last century with the
48 introduction of electric lighting. One of the consequences of the modern light environment is
49 circadian disruption, or misalignment between the internal temporal system and external cues(1).
50 Circadian disruption can promote the development of chronic diseases, such as diabetes and
51 dyslipidemia(2-5); night shift work is even categorized by the International Agency for Research
52 on Cancer as a Group 2A carcinogen, “probably carcinogenic to humans”(6). However, little is
53 known how circadian disruption affects fetal development.

54 The Developmental Origins of Health and Disease (DOHaD) hypothesis grew out of
55 research on *in utero* undernutrition and later life risk of cardiometabolic disease(7, 8). These
56 studies found that infants born with low birthweight or small for their gestational age (SGA) had
57 an increased risk of heart disease and stroke as adults(9-13). Later, the Dutch Hunger Winter
58 cohort revealed epigenetic(14) and transgenerational(15) effects of *in utero* exposure to famine
59 on offspring. DOHaD research has grown to encompass exposure to early life stress and
60 pollutants(16), such as endocrine disrupting compounds, and outcomes related to neurological
61 and hormonal programming. Light can also act as an endocrine disruptor(17); however, the
62 influence of light exposure on developmental programming has not yet been widely assessed in
63 DOHaD studies.

64 We have previously shown that developmental chronodisruption in mice (via
65 environmental light) from embryonic day 0 until weaning at 3 weeks of age has lasting effects on
66 visual and metabolic outcomes of adult offspring; in particular, mice exposed to developmental
67 circadian disruption have increased expression of retinal microglia and macrophage markers
68 accompanied with impaired visual function(18). The placenta, a neuroendocrine organ, regulates
69 *in utero* growth, including fetal neuronal growth. Communication between the placenta and fetal
70 brain, termed the placenta-brain axis(19), influences neurodevelopment. The immune system
71 plays an important role in the placenta-brain axis, and activation of placental immune signals can
72 influence development of fetal immune cells, such as microglia, in the fetal brain(20, 21).
73 Therefore, we investigated the impacts of developmental circadian disruption on overall gene
74 expression and immune cell phenotypes in the placenta. To do this, we exposed pregnant mice to
75 developmental chronodisruption and measured fetal and placenta outcomes (count, weight, sex

76 ratio), placental gene expression (RNAseq), and placental expression of immune cell markers
77 CD11b and Iba1 (immunofluorescence).

78

79 **MATERIALS and METHODS**

80 **Ethical approval**

81 All experimental procedures were approved (#V008-19) by the Institutional Animal Care
82 and Use Committee of the Atlanta Veterans Affairs Healthcare System in facilities that are
83 accredited by the Association for the Assessment and Accreditation of Laboratory Animal Care
84 International (AAALAC).

85

86 **Animal handling and experimental design**

87 Wildtype female (~3-4 weeks old) C57BL/6J mice (*Mus musculus*) were ordered from
88 Jackson Laboratories (Bar Harbor, ME, USA); wildtype male C57BL/6J mice were ordered or
89 bred in-house from mice from Jackson Laboratories. Males for breeding were singly housed
90 whereas female breeders were co-housed in large (6"x9"x18") wire-top shoebox cages in
91 standard conditions (*ad libitum* chow (Teklad Rodent Diet 2018 irradiated 2918, Envigo Teklad,
92 Madison, WI, USA), 12:12 lighting) and checked daily for well-being. After a 2 week
93 acclimation period, naïve females were randomized to either control light (CL, 12:12 light:dark)
94 or a chronodisruption (CD) light paradigm, consisting of weekly inversions of the
95 photoperiod(18, 22, 23). Light intensity was standardized across groups to be ~50-400 lux (Dual-
96 range light meter 3151CC, Traceable, Webster, TX, USA), with darkest areas at the bottom of
97 the cage under the food holder and brightest areas near the top of the cage. Females were
98 exposed to light treatments for 4 weeks prior to timed breeding; during aligned light schedules,
99 representative females from each light treatment group were introduced to the male's cage in the
100 afternoon; females were checked for plugs and returned to their home cages after 2 days.
101 Females were weighed several days later to confirm pregnancy; if not pregnant, they were placed
102 with the same male the following week for further rounds of pairing for up to 4 more weeks of
103 pre-pregnancy light treatment. Dams remained in CD or CL light treatments until tissue
104 collection at gestational day 15.5 (E15.5). While placental tissue collection was timed to be the
105 estimated E15.5 and mouse pairings occurred in a restricted time window, we did not evaluate

106 vaginal cytology or use *in vitro* fertilization, and it is therefore possible that embryonic age
107 varied by a day.

108

109 **Tissue collection**

110 Pregnant mice (E15.5) were sacrificed with compressed CO₂ gas anesthesia, followed by
111 cervical dislocation and rapid decapitation for truncal blood collection between 9AM-11AM
112 (ZT3-5); within this range, tissue collection time did not substantially differ between CL and CD
113 groups. Position of each placental sample within the uterine horns, placental wet weight, and
114 reabsorptions were recorded and placentae immediately dissected out after removing uterine
115 tissue. Placental tissue samples were snap-frozen in liquid nitrogen and stored at -80°C until
116 further processing for RNA isolation or preserved in 10% neutral buffered formalin for
117 histological and immunohistochemical analyses. Fetal tail samples were also collected, snap
118 frozen, and stored at -80°C until later use for sex determination. Samples from 3 dams, all from
119 the CD group, were excluded due to noted quality issues during collection; for example, in 2
120 mice, all of the embryos in a uterine horn exhibited blood clots and discoloration. Samples from
121 a total of 12 dams, 6 CL and 6 CD, were included in the analysis.

122

123 **RNA isolation, sequencing, alignment, and generation of count data**

124 Prior to placental RNA isolation, all fetal tail tissue samples were lysed and RNA extracted using
125 the Qiagen Allprep DNA/RNA Mini Kit according to manufacturer's instructions and *Sry* gene
126 expression measured via PCR to determine sex (*Sry*FWD: 5' – TGG GAC TGG TGA CAA TTG
127 TG -3' and *Sry*REV : 5' – GAG TAC AGG TGT GCA GCT CT-3'). Samples with faint bands
128 were re-run. For RNA sequencing, placental samples without any noted collection quality issues
129 were randomly selected and matched on sex when possible (quality samples of both sexes were
130 not available for each dam). Two samples from each dam were chosen, for a total of 24 placenta
131 samples, 12 from each light treatment group, and DNA and RNA isolated using the Qiagen
132 Allprep DNA/RNA Mini Kit according to manufacturer's instructions. RNA quality was
133 measured using the Agilent 2100 Bioanalyzer with Agilent RNA 6000 Nano kit (cat# 5067-
134 1511) following manufacturer's instructions and RNA concentrations measured with a Thermo
135 Scientific NanoDrop spectrophotometer. All samples had RIN scores ≥ 9 . Placental RNA
136 samples (n=24) were sent to the Emory Genomics core for PolyA RNA sequencing performed at

137 30M read depth. FastQC was performed to check read quality and fastq files aligned to the C57
138 mouse genome (Ensemble assembly GRCm38.p6) with STAR v2.7 using default settings. Read
139 counts were derived using the “quantmode” command in STAR. Raw sequencing data FastQ
140 files, processed gene count data, and sample information have been deposited in GEO (accession
141 number GSE169266). Code for sample alignment and processing, as well as gene count data, are
142 available at: https://github.com/dclarktown/CD_mice_placenta (DOI: 10.5281/zenodo.4536522).

143

144 **Differential expression (DE) analysis**

145 Count data were read into R (version 3.2) and analyzed for differential expression (DE)
146 using DESeq2(24). The original 53,801 transcripts measured were limited to transcripts that had
147 at least 1 count in 10% of samples, leaving a total of 14,739 transcripts for analysis. To confirm
148 sex of samples, samples were also evaluated for high expression of *Xist* mRNA, indicative of
149 female sex. Of the 24 samples, 1 sample was mismatched for sex (sample #9, 1009) and edited to
150 the correct sex. After 1 sample was found to be an outlier driving many of the DE results (sample
151 #12, 1012), it was dropped from the analysis. The DE analysis of the remaining 23 samples
152 adjusted for sex and the first surrogate variable, with developmental light treatment group as the
153 main exposure. The first surrogate variable was computed using the *sva* package(25) and “be”
154 method with 200 iterations. Results were adjusted for false discovery rate using the Benjamini
155 and Hochberg (BH) method and considered significant if $q < 0.05$.

156

157 **Pathway analysis**

158 Transcript enrichment for differentially expressed genes was performed using
159 EnrichR(26) among the Mouse Gene Atlas, ChEA 2016, KEGG 2019 Mouse, and GO 2018
160 (Biological Process, Molecular Function, Cellular Component) databases. Results were adjusted
161 for multiple comparisons using the Benjamini-Hochberg (BH) method and considered significant
162 if $q < 0.05$.

163

164 **Placental immunofluorescence measurement and quantification**

165 Fresh placenta samples were fixed in 10% neutral buffered formalin overnight at 4°C and
166 then cryoprotected the following day in 30% sucrose after washing with 1x PBS. Samples were
167 embedded and frozen in optimal cutting temperature compound and sliced into 7- μ m-thick

168 sections. Placental sections were blocked (with 0.1% Triton X-100) and incubated with primary
169 antibodies in 5% normal donkey serum in PBS before washing with PBS. Primary antibody
170 incubations using Iba1 (ab178847; 1:100; Abcam) and CD11b (14-0112-82; 1:100; Invitrogen)
171 were performed for 16-24 hours at 4°C and secondary antibody incubations were performed for 1
172 hour at room temperature using Alexa Fluor 488 Donkey anti-mouse IgG (A-21202; 1:500) and
173 Alexa Fluor 647-conjugated Donkey anti-rabbit IgG (A-31573; 1:500). Tissue nuclei were
174 visualized with nuclear stain 4',6-diamidino-2-phenylindole (DAPI, 62247; Thermo Fisher
175 Scientific). Coverslips were mounted using Prolong Gold (P36934; Thermo Fisher Scientific).
176 Placental tissue (n=4-6 mice/group; 3 images per sample, averaged for the analysis) was imaged
177 with an Olympus Fluoview1000 confocal microscope (Center Valley, PA) using a 20x objective
178 and a Lumenera INFINITY 1-3C USB 2.0 Color Microscope camera (Spectra Services, Ontario,
179 NY). All images were processed and quantified using ImageJ software by a researcher masked to
180 treatment group.

181

182 **Statistical analysis and data availability**

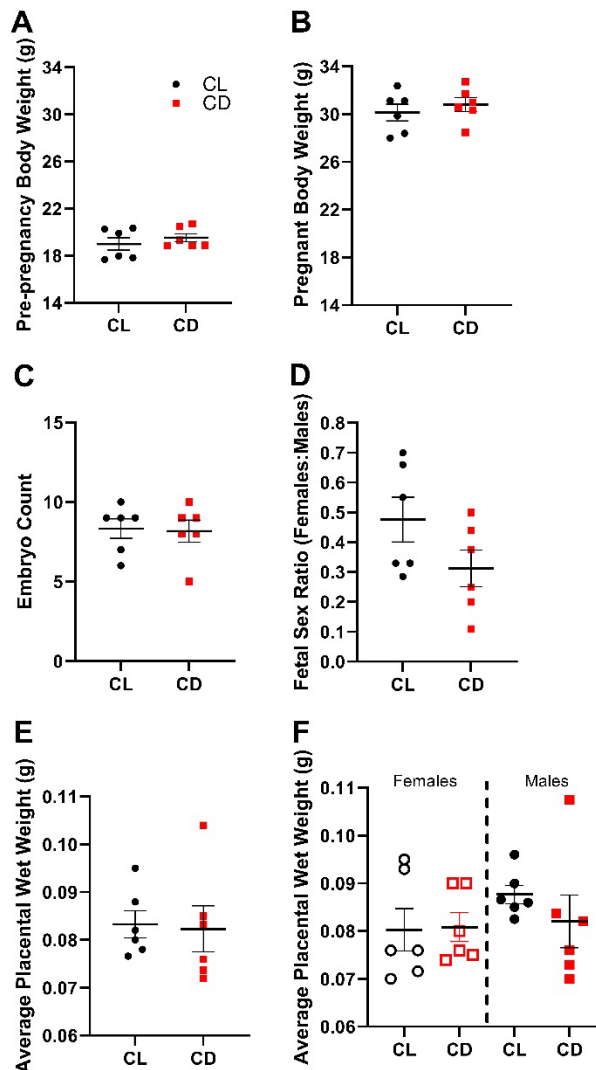
183 Unless otherwise noted, weight, embryo number, placental weight, sex ratio, and
184 immunofluorescence data were all analyzed with Student's 2-tailed unpaired t-tests and
185 considered significant if $p < 0.05$. Statistical tests were performed in Prism version 9.0.0. Statistics
186 for placental gene expression analyses are described in the previous sections. All data and code
187 used for the analyses are available at: https://github.com/dclarktown/CD_mice_placenta (DOI:
188 10.5281/zenodo.4536522), except for the raw sequencing data which has been deposited in GEO
189 (accession number GSE169266).

190

191 **RESULTS and DISCUSSION**

192 Here, we investigated whether circadian disruption led to gene expression and
193 immunologic changes in the placenta. We have previously shown that developmental CD light
194 treatment alters programming of the visual system in offspring(18). CD females did not differ in
195 pre-pregnancy weight (Student's unpaired 2-tailed t-test, $t=0.83$, $df=10$, $p=0.43$, **Figure 1A**) or
196 pregnancy weight at tissue collection (Student's unpaired 2-tailed t-test, $t=0.72$, $df=10$, $p=0.49$,
197 **Figure 1B**) compared to CL females. There were also no differences in embryo count, fetal sex
198 ratio, and placental weight (**Figure 1C-F**), consistent with previous findings(27) in a rat model

199 that additionally found no change in fetal weight or placental:fetal weight ratio. Genetic models
200 of developmental circadian disruption have found similar null results; knockout of *Bmal1*
201 (*Arntl*), a core circadian clock gene, in fetal tissue does not alter embryo number or fetal or
202 placental weight(28), whereas knockout in parental male or female tissue causes infertility(29).
203 However, the exclusion of 2 CD dams from the analysis due to discoloration and blood clots
204 throughout one uterine horn may have biased results towards a more conservative measure of
205 effect.
206



207

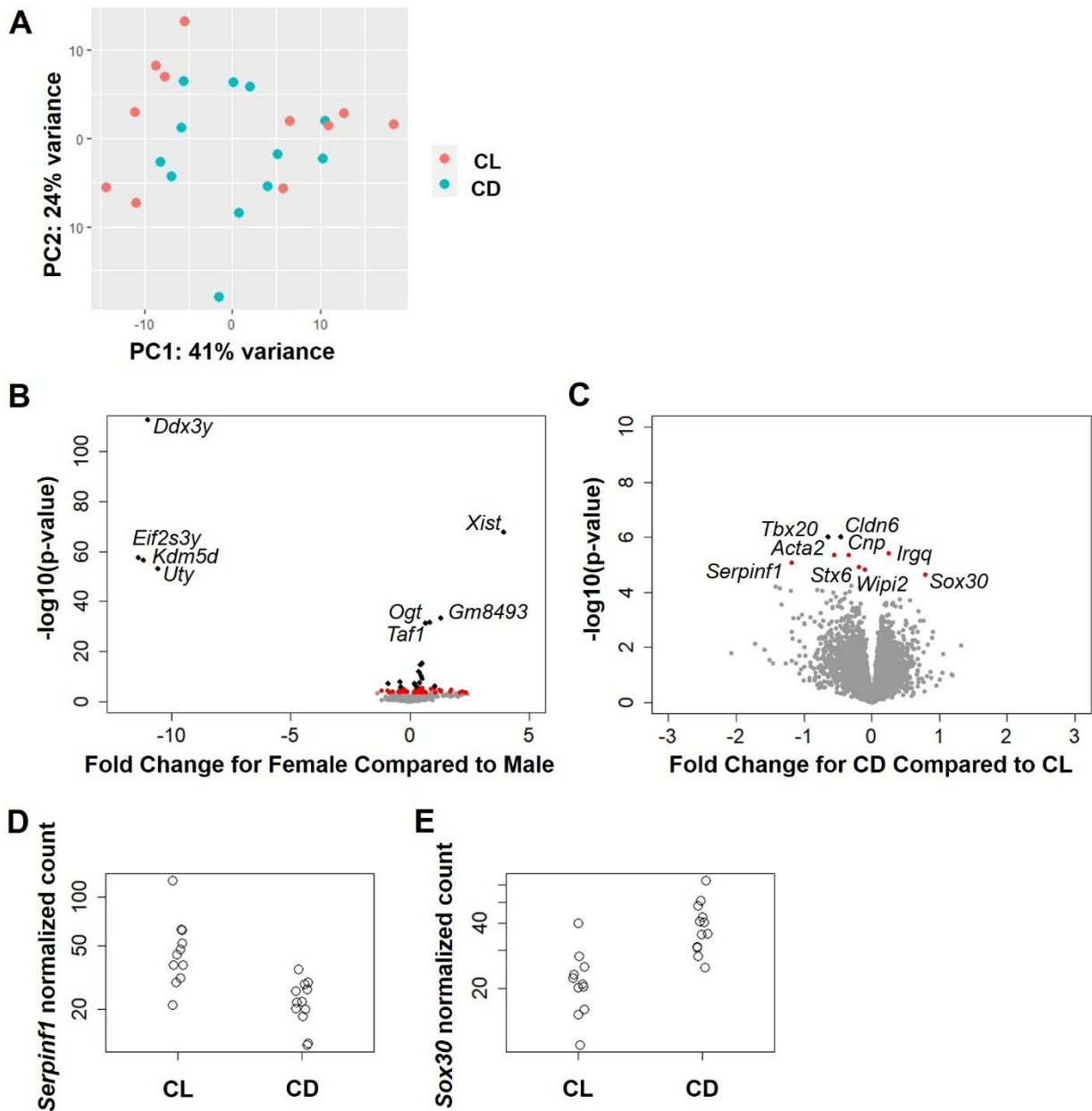
208 **Figure 1. Light treatment did not alter dam or fetal outcomes.** Body weight (grams) of
209 female mice (CL n=6, CD n=6) from which placental samples were collected (A) just prior to
210 pairing for timed breeding (Student's unpaired 2-tailed t-test, $t=0.83$, $df=10$, $p=0.43$) and (B)
211 when pregnant at E15.5 just prior to tissue collection (Student's unpaired 2-tailed t-test, $t=0.72$,

212 df=10, p=0.49). (C) Number of viable embryos per dam counted within the uterine horns
213 (Student's 2-tailed unpaired t-test, t=0.18, df=10, p=0.86). (D) Sex ratio of viable embryos per
214 dam, as determined by PCR of fetal tail snip and subset confirmed by RNA sequencing
215 (Student's 2-tailed unpaired t-test, t=1.67, df=10, p=0.12). (E) Average placental wet weight
216 (grams) per dame (Student's 2-tailed unpaired t-test, t=0.16, df=10, p=0.87). (F) Average
217 placental wet weight (grams) per dam, stratified by sex (1-way ANOVA, F (3, 20) = 0.73,
218 p=0.55). All data are presented as mean \pm SEM.

219
220 Placentas were collected at the late stage of pregnancy and sequenced for gene
221 expression. Among the most highly expressed transcripts across all placenta samples (regardless
222 of exposure) were *Tpbpa*, *Prl3b1*, *Tpbpb*, *Psg21*, *Prl8a9*, and *Psg23*, gene expression typical of
223 trophoblasts(30). The EnrichR pathway analysis of the top 100 most highly expressed placental
224 genes indicated enrichment for mouse placental tissue (q<0.05, **Supplemental File 1**) in the
225 Mouse Gene Atlas database, as expected, and, interestingly, for the CLOCK, NELFA, and HSF1
226 transcription factors in the ChEA database. CLOCK is a core component of the circadian clock,
227 and as mediator of the maternal and fetal environments, the placenta may function as a peripheral
228 oscillator; we have previously shown that placental gene expression varies seasonally(31), which
229 suggests sensitivity to seasonal environmental exposures such as light and temperature. Top
230 KEGG pathways were: "antigen processing and presentation", "protein processing in
231 endoplasmic reticulum", "lysosome" and "HIF-1 signaling pathway"; likewise, top GO pathways
232 were related to immune signaling and protein processing, with terms such as "ATF6-mediated
233 unfolded protein response", "neutrophil degranulation", "collagen binding", "secretory granule
234 lumen", and "focal adhesion" (**Supplemental File 1**).

235 Principle component analysis of the placental samples revealed relative overlap between
236 the CL and CD groups (**Figure 2A**). This pattern was not explained by sample position within
237 uterine horn, sample collection time, sex ratio, or RNA quality, and samples from the same dam
238 did not necessarily cluster together. The DE analysis between male and female placental tissue
239 (adjusting for light treatment) resulted in 77 sex-specific placental transcripts (q<0.05, **Figure**
240 **2B, Supplemental File 2**). A number of these genes were strikingly different; *Xist*, a non-coding
241 RNA that silences the extra X-chromosome in females and can be used to identify fetal sex(32),
242 was highly expressed in female placenta. *Ddx3y*, *Eif2s3y*, *Kdm5d*, and *Uty* were all highly
243 expressed in male placenta and have previously been reported as male-specific placental
244 genes(33, 34); these genes could arguably also be used to identify fetal sex. Sex-specific
245 placental gene expression (n=113 q<0.1) also displayed enrichment for pathways related to lipid,

246 retinoid, and cholesterol metabolism in the KEGG and GO term databases, suggesting sex-
247 specific regulation of these processes in the placenta (**Supplemental File 3**). Interestingly,
248 studies of maternal malnutrition and high fat diet exposure have uncovered sex-specific
249 placental(35-37) and phenotypic outcomes in the offspring(38, 39). These results support
250 investigation of these pathways in sex-specific development in future studies.
251



252

253 **Figure 2. Placental gene expression varies by sex and light treatment group.** (A) PCA plot of
254 first 2 principal components comparing treatment groups shows general overlap between CL and

255 CD groups. **(B)** Volcano plot of differential placental gene expression by sex (adjusting for light
256 treatment group and first surrogate variable). Male is the reference group, so transcripts with
257 decreased expression in females (or, conversely, increased expression in males) are located to the
258 left of 0, while transcripts with increased expression in females (or, conversely, decreased
259 expression in males) are located to the right of the 0. Black dots denote Bonferroni-significant
260 transcripts (n=22 p<0.05), red dots denote BH-significant transcripts (n=77 q<0.05), and grey
261 dots denote non-significant transcripts. The top differentially expressed genes are plotted with
262 their respective gene names. **(C)** Volcano plot of differential placental gene expression by
263 treatment (adjusting for sex and first surrogate variable). CL is the reference group, so transcripts
264 with decreased expression in CD (or, conversely, increased expression in CL) are located to the
265 left of the 0, while transcripts with increased expression in CD (or, conversely, decreased
266 expression in CL) are located to the right of the 0. Black dots denote Bonferroni-significant
267 transcripts (n=2 p<0.05), red dots denote BH-significant transcripts (n=9 q<0.05) and grey dots
268 denote non-significant transcripts. Plots of raw normalized count data for **(D)** *Serpinf1* and **(E)**
269 *Sox30* by treatment group.
270

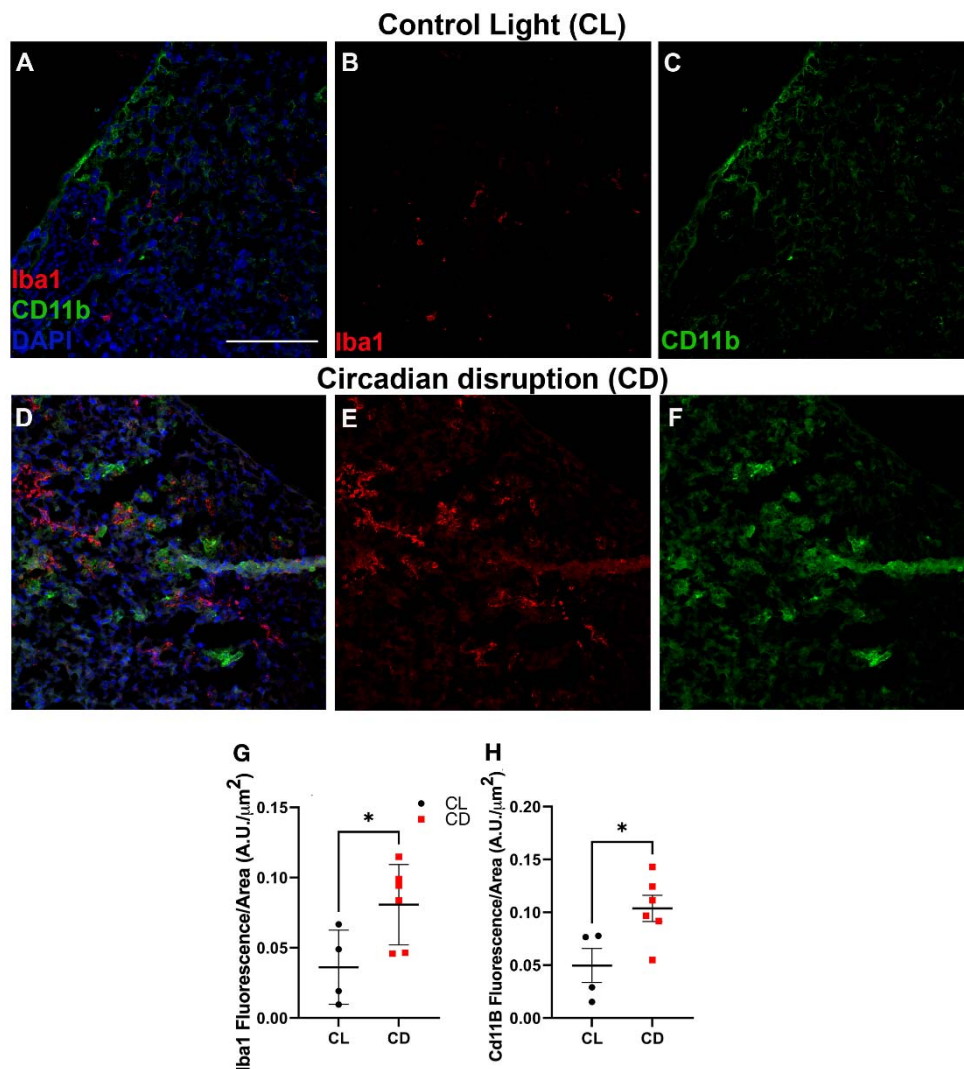
271 Few transcripts exhibited large differences between light treatment groups (**Figure 2C**).
272 However, of the differentially expressed genes (n=9 q<0.05, **Supplemental File 4**), *Serpinf1*,
273 *Tbx20*, *Acta2*, *Cldn6*, *Cnp*, *Stx6*, and *Wipi2* had decreased expression while *Sox30* and *Irgq* had
274 increased expression in CD placenta (**Figure 2C-E**). Pathway analysis revealed that
275 differentially expressed genes were similar to gene expression in osteoblasts in the Mouse Gene
276 Atlas database (**Supplemental File 5**). While there was no enrichment for specific transcription
277 factors within the ChEA database, differentially expressed genes were enriched for “cholesterol
278 metabolism” in the KEGG database and terms related to tissue development, adhesion, and
279 cytoplasmic projection in the GO databases. It is perhaps surprising that we did not uncover large
280 differences in placental gene expression between light treatment groups. However, it is possible
281 the small sample size limited the ability to measure more subtle differences in gene expression,
282 especially if such differences occurred in placental cell subpopulations, such as immune cells.

283 Placenta from CD-exposed dams revealed significantly increased expression of Iba1 and
284 CD11b microglial/macrophage markers than placenta from dams housed in CL conditions
285 (p=0.027 and p=0.038, respectively, **Figure 3**). These results align with the finding of decreased
286 *Serpinf1* (which encodes pigment epithelium-derived factor (PEDF)) expression in CD placenta.
287 A neurotrophic factor with many roles(40), PEDF inhibits macrophage inflammatory
288 processes(41), which may have contributed to the increased CD11b and Iba1 marker expression
289 in CD placenta. These data also coincide with our findings of an increased retinal inflammatory
290 response and reduced visual function within mice developmentally exposed to CD(18). The

291 immune system and inflammation govern many of the health outcomes caused by chronic
292 circadian disruption(42-44). For example, night shift workers were found to have greater
293 amounts of immune cells, such as T cells and monocytes, than non-shift workers(45); likewise,
294 we previously reported hypomethylation in immune-related genes, such as *CLEC16A*, *SMPD1*,
295 and *TAPBP*, in the placentas of mothers who worked the night shift(46). In rodent studies,
296 chronic circadian disruption increased macrophages and “pro-tumor” CD11b+ MHCII cells(47),
297 altered inflammatory response in the brain(48), and primed the innate immune response to be
298 more pro-inflammatory(49).

299 The placenta is the only organ formed by the interaction of both fetal/embryonic and
300 maternal tissues and acts as the interface between both circulatory systems(50). Previous
301 research has found a strong correlation between placental CD11b expression and fetal brain
302 microglial activation(21). In mice and humans, brain and placental macrophages and microglia
303 originally derive from the same source: the fetal yolk sac(51, 52). These progenitor macrophage
304 and microglial cells migrate from the yolk sac to embryonic tissues, where they set up residence;
305 once settled, they are long-lived and able to replenish themselves(53, 54). Our results suggest
306 that developmental light environment affects programming of the placental and fetal immune
307 systems, laying the groundwork for a pro-inflammatory setting later in life. These findings
308 provide novel evidence linking CD with increased placental inflammatory response and highlight
309 the need to evaluate the influence of the light environment on health and disease outcomes in
310 DOHaD studies.

311



312
 313 **Figure 3. Chronodisruption causes increased macrophage and microglial signaling in the**
 314 **placenta.** Placentas from (A-C) control light (CL) and mice exposed to (D-F) developmental
 315 circadian disruption (CD) were labeled for inflammatory markers labeling microglia and
 316 macrophages. In placenta from CD mice increased placental (G) Iba1 fluorescence (Student's 2-
 317 tailed unpaired t-test, $t=2.49$, $df=8$, $p=0.038$) and increased placental (H) CD11b fluorescence
 318 (Student's 2-tailed unpaired t-test, $t=2.70$, $df=8$, $p=0.027$) were detected. CL=4 placenta from
 319 different dams, 3 images each; CD=6 placenta from different dams, 3 images each. All data are
 320 presented as mean \pm SEM, scale bar = 20 microns, and $*=p<0.05$.

321
 322 **Acknowledgements**

323 This work was supported by funding from the National Institutes of Health (NIH-NICHD F31
 324 HD097918 [to DACT], NIH-NIEHS T32 ES012870 [to DACT], NIH-NIEHS P30ES019776 [to
 325 CJM], NIH-NEI Core Grant P30EY006360) and the Department of Veterans Affairs

326 (Rehabilitation Research and Development Senior Research Career Scientist Award RX003134
327 [to MTP]. This study was supported in part by the Emory Integrated Genomics Core (EIGC),
328 which is subsidized by the Emory University School of Medicine and is one of the Emory
329 Integrated Core Facilities. Additional support was provided by the Georgia Clinical &
330 Translational Science Alliance of the National Institutes of Health under Award Number
331 UL1TR002378. The sequencing for this study was supported in part by the Emory Molecules to
332 Mankind (M2M) program, funded by the Burroughs Wellcome Fund. The study sponsors did not
333 have any role in the study design, collection, analysis, interpretation of the data, writing of the
334 report, or the decision to submit the paper for publication.

335

336 **Author Contributions**

337 D. Clarkson-Townsend designed the study, performed the experiments, analyzed the data, and
338 wrote and edited the manuscript. K. Bales stained, imaged, quantified, and analyzed placenta
339 samples for immunofluorescence and contributed to writing and editing of the manuscript. K.
340 Hermetz contributed to sample preparation and measurement for mRNA sequencing and editing
341 of the manuscript. A. Burt contributed to genome alignment of sequencing data and editing of
342 the manuscript. M. Pardue provided experimental resources and contributed to experimental
343 design and editing of the manuscript. C. Marsit contributed to experimental design and editing of
344 the manuscript.

345

346 **References**

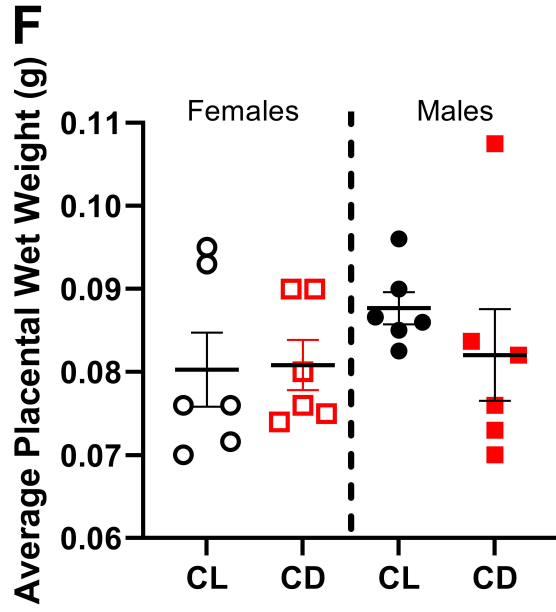
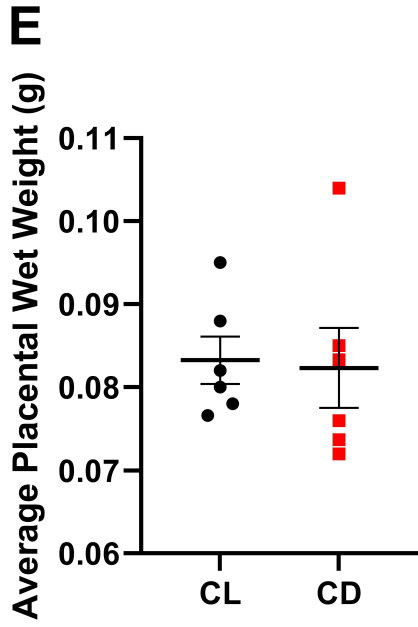
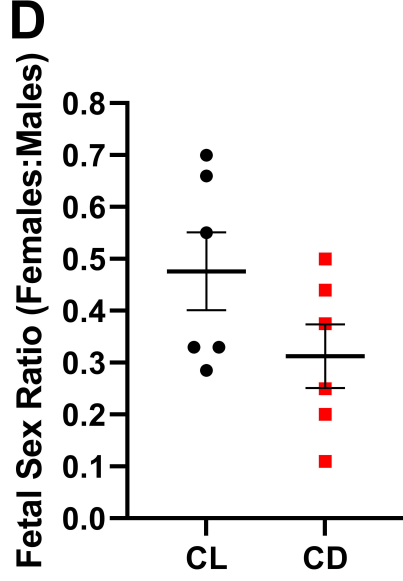
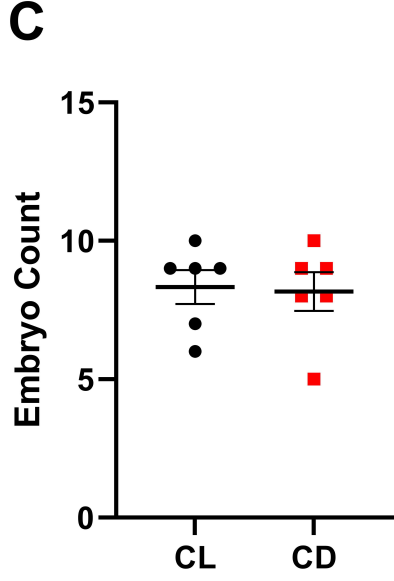
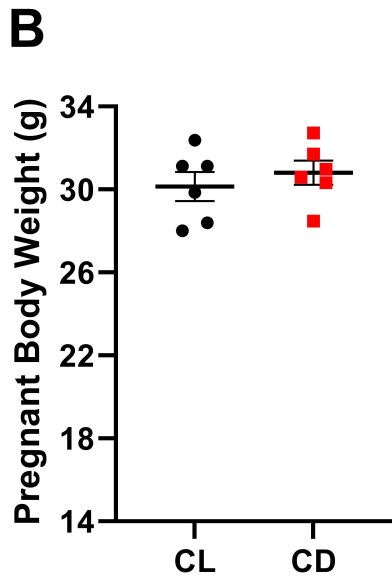
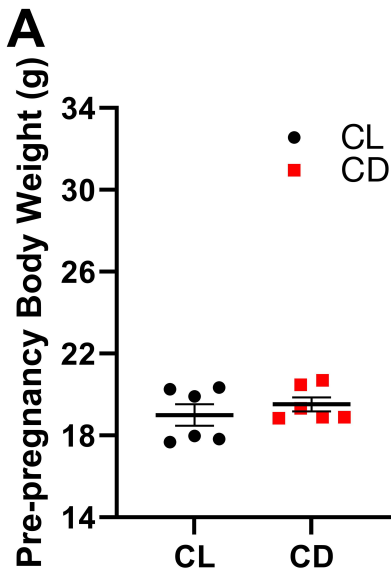
- 347 1. Lunn RM, Blask DE, Coogan AN, Figueiro MG, Gorman MR, Hall JE, et al. Health
348 consequences of electric lighting practices in the modern world: A report on the National Toxicology
349 Program's workshop on shift work at night, artificial light at night, and circadian disruption. *Sci Total*
350 *Environ.* 2017;607-608:1073-84.
- 351 2. Reutrakul S, Knutson KL. Consequences of Circadian Disruption on Cardiometabolic Health.
352 *Sleep Med Clin.* 2015;10(4):455-68.
- 353 3. Shimba S, Ogawa T, Hitosugi S, Ichihashi Y, Nakadaira Y, Kobayashi M, et al. Deficient of a
354 Clock Gene, Brain and Muscle Arnt-Like Protein-1 (BMAL1), Induces Dyslipidemia and Ectopic Fat
355 Formation. *PLOS ONE.* 2011;6(9):e25231.
- 356 4. Morris CJ, Yang JN, Garcia JI, Myers S, Bozzi I, Wang W, et al. Endogenous circadian system
357 and circadian misalignment impact glucose tolerance via separate mechanisms in humans. *Proceedings of*
358 *the National Academy of Sciences.* 2015;112(17):E2225-E34.
- 359 5. Karatsoreos IN, Bhagat S, Bloss EB, Morrison JH, McEwen BS. Disruption of circadian clocks
360 has ramifications for metabolism, brain, and behavior. *Proceedings of the National Academy of Sciences.*
361 2011;108(4):1657-62.
- 362 6. IARC. Carcinogenicity of night shift work. *Lancet Oncol.* 2019;20(8):1058-9.

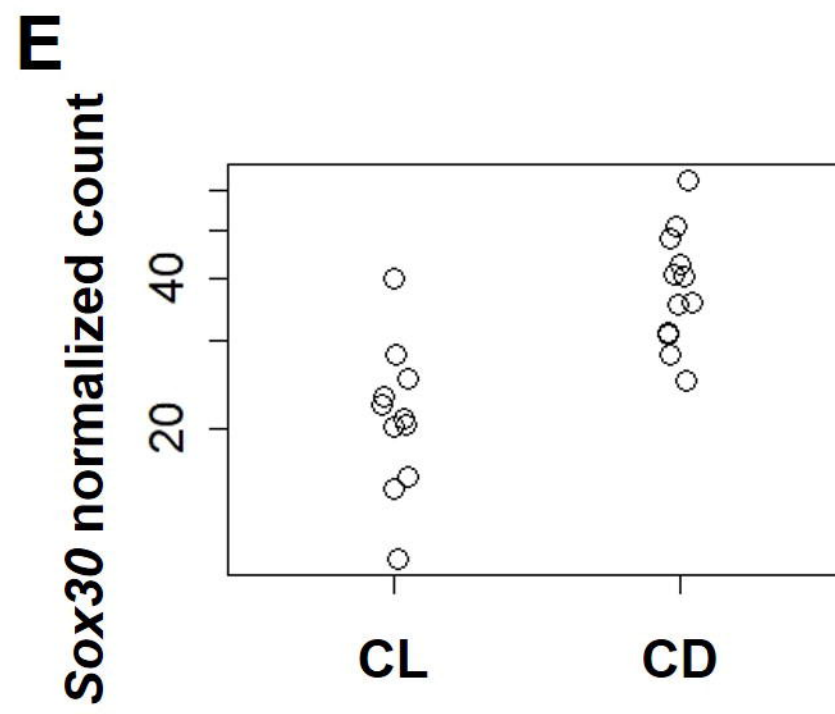
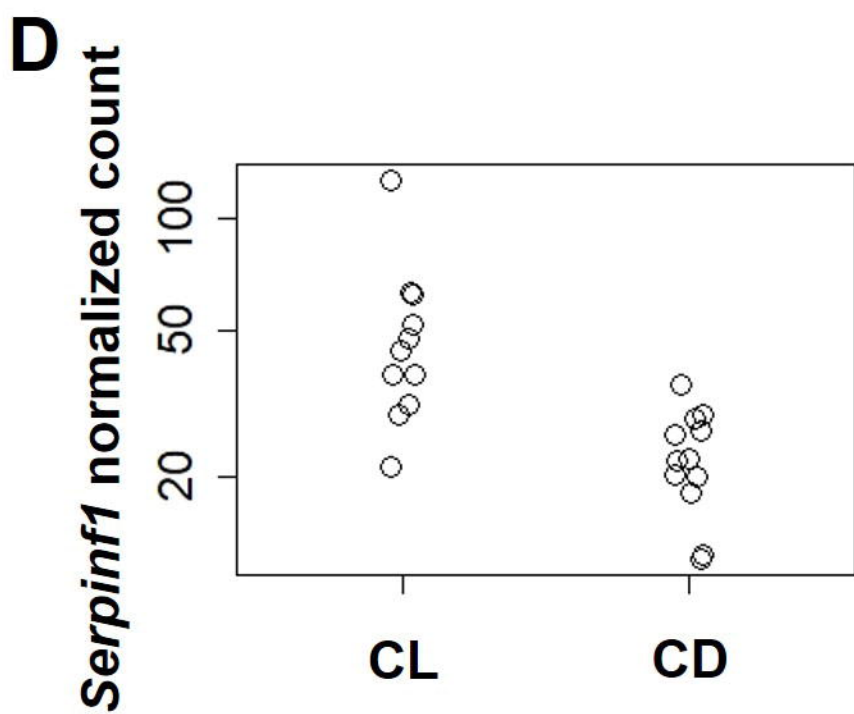
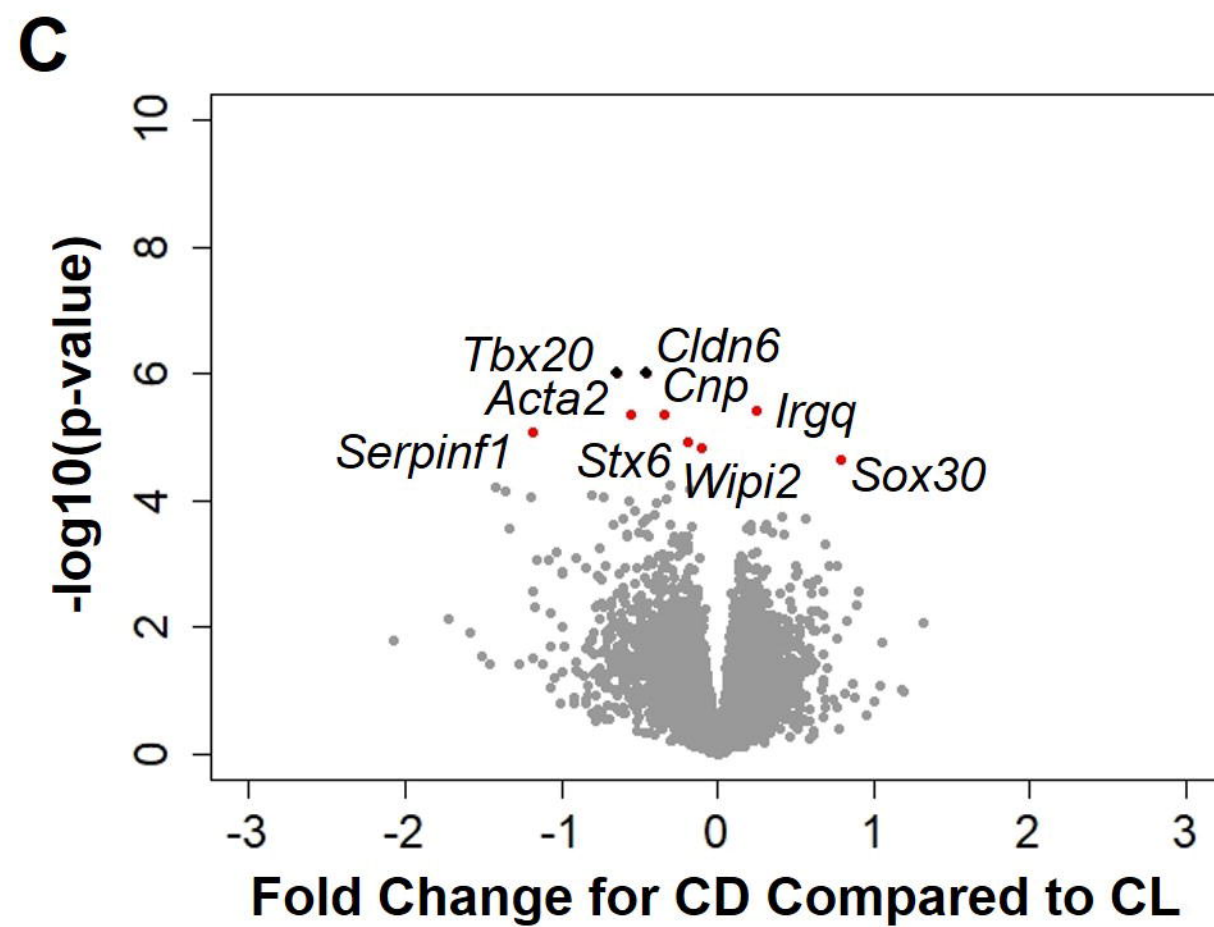
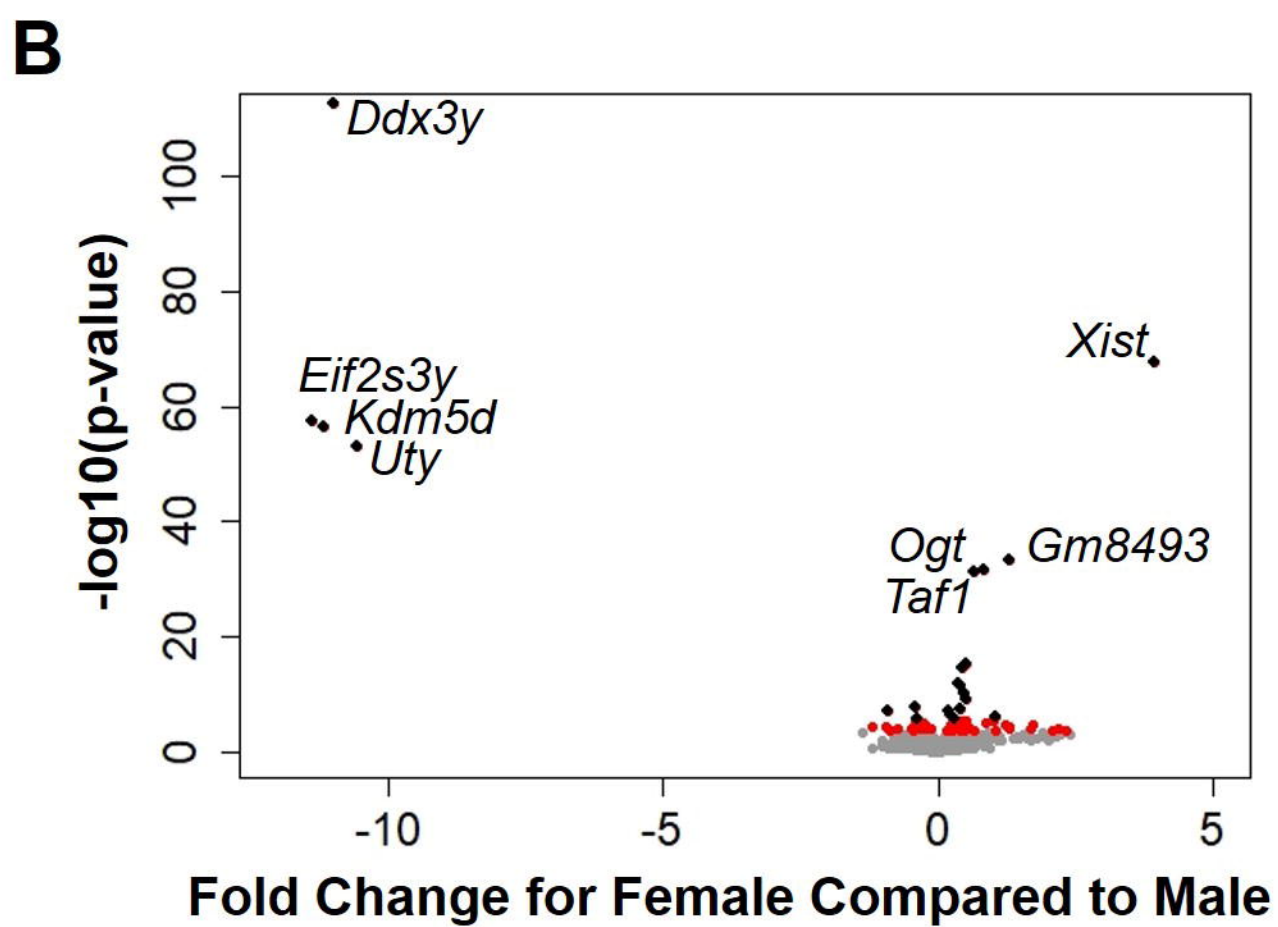
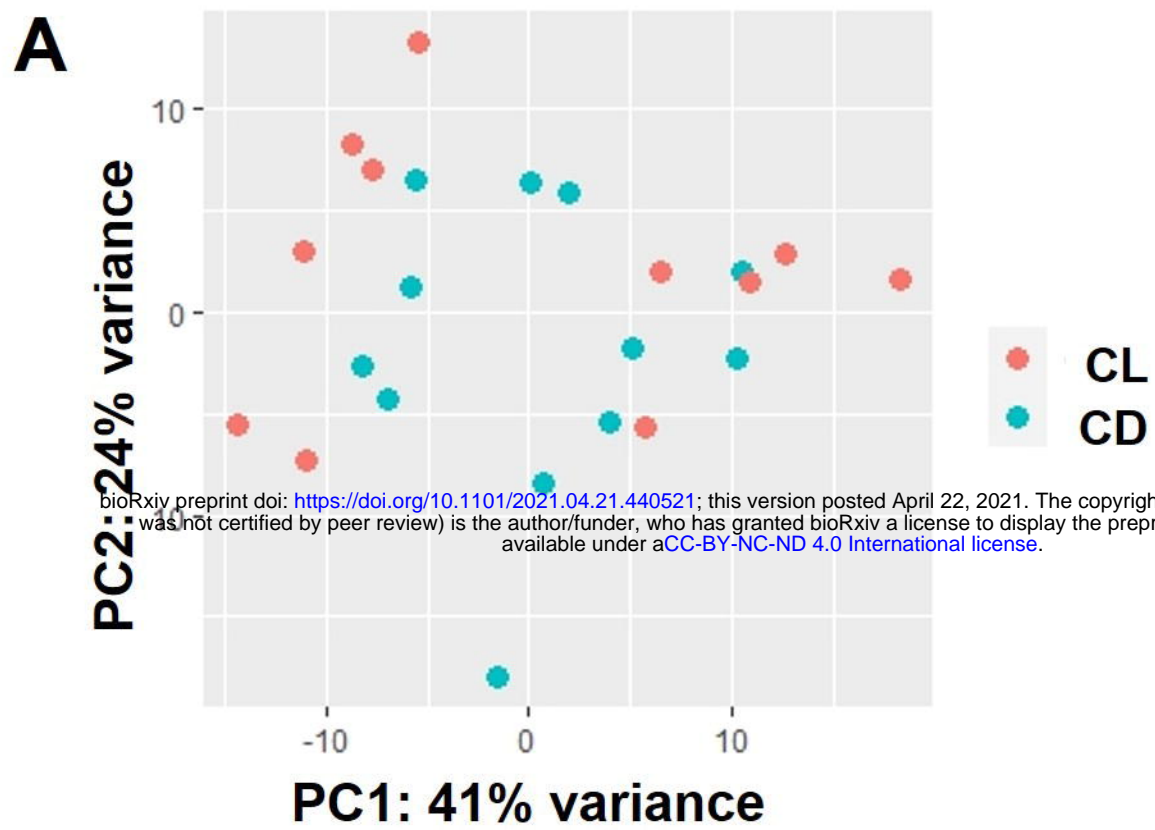
- 363 7. Barker DJ, Osmond C. Infant mortality, childhood nutrition, and ischaemic heart disease in
364 England and Wales. *Lancet*. 1986;1(8489):1077-81.
- 365 8. Barker DJP. The Developmental Origins of Adult Disease. *Journal of the American College of*
366 *Nutrition*. 2004;23(sup6):588S-95S.
- 367 9. Rich-Edwards JW, Stampfer MJ, Manson JE, Rosner B, Hankinson SE, Colditz GA, et al. Birth
368 weight and risk of cardiovascular disease in a cohort of women followed up since 1976. *Bmj*.
369 1997;315(7105):396-400.
- 370 10. Osmond C, Barker DJ, Winter PD, Fall CH, Simmonds SJ. Early growth and death from
371 cardiovascular disease in women. *Bmj*. 1993;307(6918):1519-24.
- 372 11. Tian J, Qiu M, Li Y, Zhang Xe, Wang H, Sun S, et al. Contribution of birth weight and adult
373 waist circumference to cardiovascular disease risk in a longitudinal study. *Scientific Reports*.
374 2017;7(1):9768.
- 375 12. Wang T, Tang Z, Yu X, Gao Y, Guan F, Li C, et al. Birth Weight and Stroke in Adult Life:
376 Genetic Correlation and Causal Inference With Genome-Wide Association Data Sets. *Frontiers in*
377 *Neuroscience*. 2020;14(479).
- 378 13. Barker DJ, Gluckman PD, Godfrey KM, Harding JE, Owens JA, Robinson JS. Fetal nutrition and
379 cardiovascular disease in adult life. *Lancet*. 1993;341(8850):938-41.
- 380 14. Heijmans BT, Tobi EW, Stein AD, Putter H, Blauw GJ, Susser ES, et al. Persistent epigenetic
381 differences associated with prenatal exposure to famine in humans. *Proceedings of the National Academy*
382 *of Sciences of the United States of America*. 2008;105(44):17046-9.
- 383 15. Painter R, Osmond C, Gluckman P, Hanson M, Phillips D, Roseboom T. Transgenerational
384 effects of prenatal exposure to the Dutch famine on neonatal adiposity and health in later life. *BJOG: An*
385 *International Journal of Obstetrics & Gynaecology*. 2008;115(10):1243-9.
- 386 16. Haugen AC, Schug TT, Collman G, Heindel JJ. Evolution of DOHaD: the impact of
387 environmental health sciences. *Journal of developmental origins of health and disease*. 2015;6(2):55-64.
- 388 17. Russart KLG, Nelson RJ. Light at night as an environmental endocrine disruptor. *Physiology &*
389 *behavior*. 2018;190:82-9.
- 390 18. Clarkson-Townsend DA, Bales KL, Marsit CJ, Pardue MT. Light Environment Influences
391 Developmental Programming of the Metabolic and Visual Systems in Mice. *Investigative Ophthalmology*
392 *& Visual Science*. 2021;62(4):22-.
- 393 19. Rosenfeld CS. The placenta-brain-axis. *J Neurosci Res*. 2021;99(1):271-83.
- 394 20. Prins JR, Eskandar S, Eggen BJL, Scherjon SA. Microglia, the missing link in maternal immune
395 activation and fetal neurodevelopment; and a possible link in preeclampsia and disturbed
396 neurodevelopment? *J Reprod Immunol*. 2018;126:18-22.
- 397 21. Edlow AG, Glass RM, Smith CJ, Tran PK, James K, Bilbo S. Placental Macrophages: A Window
398 Into Fetal Microglial Function in Maternal Obesity. *International Journal of Developmental*
399 *Neuroscience*. 2019;77:60-8.
- 400 22. Mendez N, Halabi D, Spichiger C, Salazar ER, Vergara K, Alonso-Vasquez P, et al. Gestational
401 Chronodisruption Impairs Circadian Physiology in Rat Male Offspring, Increasing the Risk of Chronic
402 Disease. *Endocrinology*. 2016;157(12):4654-68.
- 403 23. Varcoe TJ, Wight N, Voultzios A, Salkeld MD, Kennaway DJ. Chronic Phase Shifts of the
404 Photoperiod throughout Pregnancy Programs Glucose Intolerance and Insulin Resistance in the Rat.
405 *PLOS ONE*. 2011;6(4):e18504.
- 406 24. Love MI, Huber W, Anders S. Moderated estimation of fold change and dispersion for RNA-seq
407 data with DESeq2. *Genome Biology*. 2014;15(12):550.
- 408 25. Leek JT, Johnson WE, Parker HS, Jaffe AE, Storey JD. The sva package for removing batch
409 effects and other unwanted variation in high-throughput experiments. *Bioinformatics*. 2012;28(6):882-3.
- 410 26. Kuleshov MV, Jones MR, Rouillard AD, Fernandez NF, Duan Q, Wang Z, et al. Enrichr: a
411 comprehensive gene set enrichment analysis web server 2016 update. *Nucleic Acids Res*.
412 2016;44(W1):W90-W7.

- 413 27. Varcoe TJ, Boden MJ, Voultzios A, Salkeld MD, Rattanatray L, Kennaway DJ. Characterisation
414 of the Maternal Response to Chronic Phase Shifts during Gestation in the Rat: Implications for Fetal
415 Metabolic Programming. *PLOS ONE*. 2013;8(1):e53800.
- 416 28. Varcoe TJ, Gatford KL, Kennaway DJ. Maternal circadian rhythms and the programming of adult
417 health and disease. *American journal of physiology Regulatory, integrative and comparative physiology*.
418 2018;314(2):R231-r41.
- 419 29. Alvarez JD, Hansen A, Ord T, Bebas P, Chappell PE, Giebultowicz JM, et al. The circadian clock
420 protein BMAL1 is necessary for fertility and proper testosterone production in mice. *Journal of biological*
421 *rhythms*. 2008;23(1):26-36.
- 422 30. Marsh B, Blelloch R. Single nuclei RNA-seq of mouse placental labyrinth development. *eLife*.
423 2020;9:e60266.
- 424 31. Clarkson-Townsend DA, Kennedy E, Everson TM, Deyssenroth MA, Burt AA, Hao K, et al.
425 Seasonally variant gene expression in full-term human placenta. *The FASEB Journal*. 2020;34(8):10431-
426 42.
- 427 32. Hoch D, Novakovic B, Cvitic S, Saffery R, Desoye G, Majali-Martinez A. Sex matters: XIST and
428 DDX3Y gene expression as a tool to determine fetal sex in human first trimester placenta. *Placenta*.
429 2020;97:68-70.
- 430 33. Gabory A, Ferry L, Fajardy I, Jouneau L, Gothié J-D, Vigé A, et al. Maternal diets trigger sex-
431 specific divergent trajectories of gene expression and epigenetic systems in mouse placenta. *PloS one*.
432 2012;7(11):e47986-e.
- 433 34. Lee J-Y, Yun HJ, Kim CY, Cho YW, Lee Y, Kim MH. Prenatal exposure to dexamethasone in
434 the mouse induces sex-specific differences in placental gene expression. *Development, Growth &*
435 *Differentiation*. 2017;59(6):515-25.
- 436 35. Mao J, Zhang X, Sieli PT, Falduto MT, Torres KE, Rosenfeld CS. Contrasting effects of different
437 maternal diets on sexually dimorphic gene expression in the murine placenta. *Proceedings of the National*
438 *Academy of Sciences of the United States of America*. 2010;107(12):5557-62.
- 439 36. Gallou-Kabani C, Gabory A, Tost J, Karimi M, Mayeur S, Lesage J, et al. Sex- and Diet-Specific
440 Changes of Imprinted Gene Expression and DNA Methylation in Mouse Placenta under a High-Fat Diet.
441 *PLOS ONE*. 2010;5(12):e14398.
- 442 37. Lin Y-J, Huang L-T, Tsai C-C, Sheen J-M, Tiao M-M, Yu H-R, et al. Maternal high-fat diet sex-
443 specifically alters placental morphology and transcriptome in rats: Assessment by next-generation
444 sequencing. *Placenta*. 2019;78:44-53.
- 445 38. Nguyen LT, Chen H, Pollock C, Saad S. SIRT1 reduction is associated with sex-specific
446 dysregulation of renal lipid metabolism and stress responses in offspring by maternal high-fat diet.
447 *Scientific reports*. 2017;7(1):8982.
- 448 39. Howie GJ, Sloboda DM, Vickers MH. Maternal undernutrition during critical windows of
449 development results in differential and sex-specific effects on postnatal adiposity and related metabolic
450 profiles in adult rat offspring. *The British journal of nutrition*. 2012;108(2):298-307.
- 451 40. Tombran-Tink J, Barnstable CJ. PEDF: a multifaceted neurotrophic factor. *Nature Reviews*
452 *Neuroscience*. 2003;4(8):628-36.
- 453 41. Zamiri P, Masli S, Streilein JW, Taylor AW. Pigment Epithelial Growth Factor Suppresses
454 Inflammation by Modulating Macrophage Activation. *Investigative Ophthalmology & Visual Science*.
455 2006;47(9):3912-8.
- 456 42. Comas M, Gordon CJ, Oliver BG, Stow NW, King G, Sharma P, et al. A circadian based
457 inflammatory response – implications for respiratory disease and treatment. *Sleep Science and Practice*.
458 2017;1(1):18.
- 459 43. Inokawa H, Umemura Y, Shimba A, Kawakami E, Koike N, Tsuchiya Y, et al. Chronic circadian
460 misalignment accelerates immune senescence and abbreviates lifespan in mice. *Scientific reports*.
461 2020;10(1):2569.

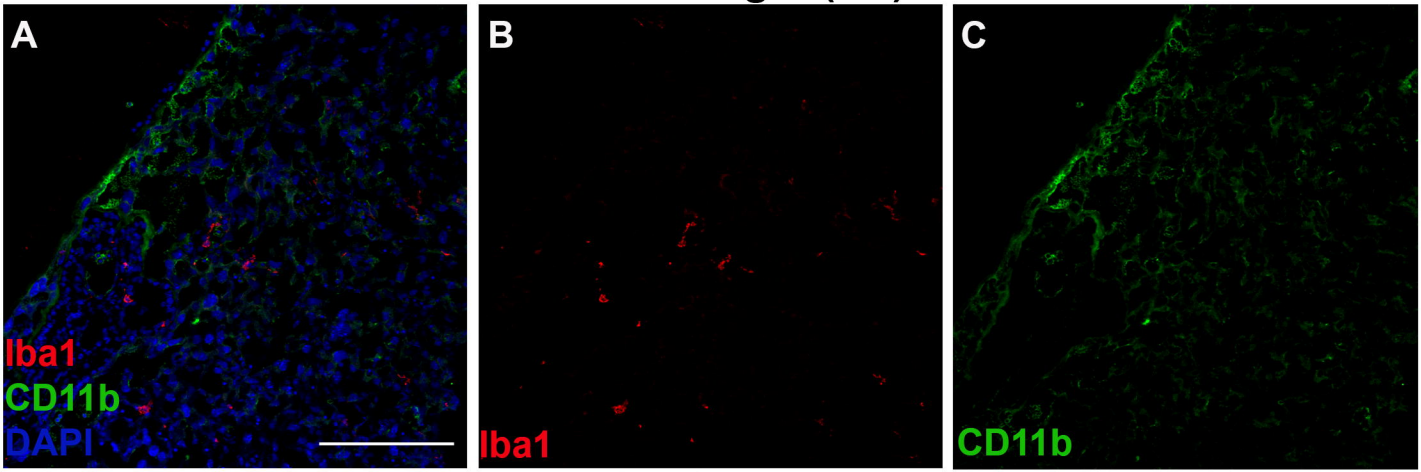
- 462 44. Castanon-Cervantes O, Wu M, Ehlen JC, Paul K, Gamble KL, Johnson RL, et al. Dysregulation
463 of inflammatory responses by chronic circadian disruption. *Journal of immunology (Baltimore, Md :*
464 *1950)*. 2010;185(10):5796-805.
- 465 45. Loef B, Nanlohy NM, Jacobi RHJ, van de Ven C, Mariman R, van der Beek AJ, et al.
466 Immunological effects of shift work in healthcare workers. *Scientific Reports*. 2019;9(1):18220.
- 467 46. Clarkson-Townsend DA, Everson TM, Deyssenroth MA, Burt AA, Hermetz KE, Hao K, et al.
468 Maternal circadian disruption is associated with variation in placental DNA methylation. *PloS one*.
469 2019;14(4):e0215745-e.
- 470 47. Hadadi E, Taylor W, Li X-M, Aslan Y, Villote M, Rivière J, et al. Chronic circadian disruption
471 modulates breast cancer stemness and immune microenvironment to drive metastasis in mice. *Nature*
472 *Communications*. 2020;11(1):3193.
- 473 48. Ramsey AM, Stowie A, Castanon-Cervantes O, Davidson AJ. Environmental Circadian
474 Disruption Increases Stroke Severity and Dysregulates Immune Response. *Journal of biological rhythms*.
475 2020;35(4):368-76.
- 476 49. Castanon-Cervantes O, Wu M, Ehlen JC, Paul K, Gamble KL, Johnson RL, et al. Dysregulation
477 of inflammatory responses by chronic circadian disruption. *Journal of immunology (Baltimore, Md :*
478 *1950)*. 2010;185(10):5796-805.
- 479 50. Astiz M, Oster H. Feto-Maternal Crosstalk in the Development of the Circadian Clock System.
480 *Front Neurosci*. 2020;14:631687.
- 481 51. Stremmel C, Schuchert R, Wagner F, Thaler R, Weinberger T, Pick R, et al. Yolk sac
482 macrophage progenitors traffic to the embryo during defined stages of development. *Nature*
483 *Communications*. 2018;9(1):75.
- 484 52. Godin I, Cumano A. The hare and the tortoise: an embryonic haematopoietic race. *Nat Rev*
485 *Immunol*. 2002;2(8):593-604.
- 486 53. Sieweke MH, Allen JE. Beyond stem cells: self-renewal of differentiated macrophages. *Science*.
487 2013;342(6161):1242974.
- 488 54. Ginhoux F, Schultze JL, Murray PJ, Ochando J, Biswas SK. New insights into the
489 multidimensional concept of macrophage ontogeny, activation and function. *Nat Immunol*.
490 2016;17(1):34-40.

491





Control Light (CL)



Circadian disruption (CD)

